Molecular Neurobiology

ISSN0893-7648/94/9(1–3): 93–106/$6.80

PD 142676 (CI 1002), A Novel Anticholinesterase and Muscarinic Antagonist

Mark R. Emmerling,* Vlad E. Gregor, Roy D. Schwarz, Jeff D. Scholten, Michael J. Callahan, Chitase Lee, Catherine J. Moore, Charlotte Raby, William J. Lipinski, and Robert E. Davis

Parke-Davis, Pharmaceutical Research, Division of Warner-Lambert, Ann Arbor, MI 48106

Abstract

Inhibition of brain acetylcholinesterase (AChE) can provide relief from the cognitive loss associated with Alzheimer's disease (AD). However, unwanted peripheral side effects often limit the usefulness of the available anticholinesterases. Recently, we identified a dihydroquinazoline compound, PD 142676 (CI 1002) that is a potent anticholinesterase and a functional muscarinic antagonist at higher concentrations. Peripherally, PD 142676, unlike other anticholinesterases, inhibits gastrointestinal motility in rats, an effect consistent with its muscarinic antagonist properties. Centrally, the compound acts as a cholinomimetic. In rats, PD 142676 decreases core body temperature. It also increases neocortical arousal, as measured by quantitative electroencephalography, and cortical acetylcholine levels, measured by in vivo microdialysis. The compound improves the performance of C57/B10j mice in a water maze task and of aged rhesus monkeys in a delayed match-to-sample task involving short-term memory. The combined effect of AChE inhibition and muscarinic antagonism distinguishes PD 142676 from other anticholinesterases, and may be useful in treating the cognitive dysfunction of AD and produce fewer peripheral side effects.

Index Entries: Anticholinesterase; Alzheimer's disease; cholinesterase inhibition; tacrine; enzymology; dementia; cognition; memory; treatment; cholinomimetic; centrally active; cholinergic hypothesis.

Introduction

Alzheimer's disease (AD) is accompanied by a progressive deterioration of cognitive function that eventually leads to the incapacitation of the afflicted individual *(1)*. Currently, the number of AD patients is about 4 million in the US alone, with that number expected to rise as the average lifespan of the population increases. The number of people affected by this illness, and its associated impact on family and society, makes AD one of the most pressing health problems of our time. The seminal event in the pathogenesis of AD appears to be the formation of amyloid plaques, composed primarily of β-amyloid (A/β4), a peptide of 39–42 amino acids *(2)*. The A/β4 peptide is derived from a larger protein, the amyloid precursor protein (APP). The events that lead to the formation of A/β4 and the effects of A/β4 on

*Author to whom all correspondence and reprint requests should be addressed.

nervous tissue are under intense investigation. Unfortunately, it is unlikely that we will find a treatment either to cure or to halt the progression of AD in the near future. Thus, current strategies focus on palliative treatments to mitigate the effects of AD on cognition.

One approach to treat AD is replacement therapy with cholinomimetics *(3–5)*. A number of biochemical and morphological changes occur in neurotransmitter systems of the AD brain that may contribute to the cognitive decline. The most prominent is a decrease in the forebrain cholinergic system. The levels of acetylcholine and of the cholinergic enzymes, choline acetylcholinesterase and acetylcholinesterase (AChE), decrease in the neocortex and hippocampus of the AD brain. This decrease correlates with the loss/atrophy of cholinergic nerve cells in the nucleus of Meynert of the basal forebrain, and its innervation to the neocortex and hippocampus. Functional studies show that animals with lesions to the nucleus of Meynert or to the hippocampus have impaired cognition. Also, pharmacological studies in animals, as well as humans, show that scopolamine, an antagonist of muscarinic receptors, also causes memory deficits. Cholinomimetics ameliorate the cognitive impairment, produced by lesions or scopolamine. Collectively, these observations have given rise to the "cholinergic deficit hypothesis" that postulates that loss of the cholinergic innervation to the neocortex and hippocampus is responsible for the cognitive decline in AD.

Cholinesterase inhibitors provide one means to enhance central cholinergic function. These agents increase the level of brain ACh by inhibiting its degradation, the consequence of which is to enhance chemical transmission at cholinergic synapses. Treatments with cholinesterase inhibitors such as physostigmine and tetrahydroaminoacridine (tacrine, THA, and Cognex®) show promise in improving the memory of AD sufferers *(6)*. Recent clinical trials with tacrine show especially significant improvement in the cognitive function of AD patients treated for several months *(7,8)*. It is clear from these studies that manipulation of central cholinergic function using anticholinesterases offers some relief to patients afflicted with AD.

Unfortunately, treatment with tacrine is not without its limitations. The compound can produce peripheral cholinergic side effects (e.g., diaphoresis, nausea, and diarrhea) at high doses *(6)*. Moreover, tacrine in some AD individuals can elevate the serum levels of liver enzymes *(7,8)*. Although the increase raises concern of hepatocellular damage, the serum levels of liver aminotransferases return to normal on discontinuing treatment, with no evident liver dysfunction. Tacrine also interacts with a variety of other enzymes and receptors *(9)* that have been suggested to affect tacrine's therapeutic utility. However, in most cases these interactions occur at levels of tacrine that are unlikely to be achieved in the central nervous system.

A number of new anticholinesterases are currently under consideration for the treatment of AD *(10)*. These include analogs of tacrine and of physostigmine, and several novel drugs such as huperzine A, galanthamine, metrifonate, and E2020. These compounds are in various stages of development and their efficacy in the treatment of AD remains to be tested. However, none of these anticholinesterases are the product of efforts to improve on an anticholinesterase (i.e., tacrine) already known to be effective in ameliorating the symptoms of AD. The goal of our work has been to develop a "second generation" inhibitor that possesses the anticholinesterase properties of tacrine in vitro and in vivo, while eliminating unwanted effects.

In this paper, we review the in vitro and in vivo pharmacological properties of a novel anticholinesterase PD 142676 (1,3-dichloro-6,7,8,9,10,12-hexahydroazepino[2,1-b]quinazoline). Our results indicate that PD 142676 (CI 1002) inhibits AChE like tacrine, but is unique in that it also acts as a muscarinic antagonist in the periphery, but not the central nervous system, at doses that improve cognitive performance. We expect that these properties will improve the safety and therapeutic potential of PD 142676 for the treatment of AD compared to other anticholinesterases.

Material and Methods

Chemicals

Electrophorus electricus (Type V-S) and human red blood cell (Type XIII) AChE were obtained from Sigma (St. Louis, MO).

Determination of Cholinesterase Activity

Compounds were tested for their ability to inhibit eel or human red blood cell AChE activity. The modified radiometric AChE assay of Johnson

and Russell *(11)*, as described earlier *(12)*, was used for the determinations of IC_{50} values, with ACh chloride, [acetyl-^{3}H] from New England Nuclear (Boston, MA) (specific activity of 90 mCi/mmole) as substrate. The concentration of inhibitor producing 50% inhibition of AChE activity (IC_{50}) was determined graphically, using data derived from triplicate determinations of enzyme inhibition by at least six different inhibitor concentrations, ranging from 100 μ*M* to 1 m*M*. Butyrylcholinesterase (BuChE) activity was determined by the microplate colorimetric Ellman assay *(13)* using 1 m*M* butyrylthiocholine as substrate. The assays were done in triplicate and read using a Molecular Devices (Menlo Park, CA) Thermomax microplate reader set at 405 nm.

A microplate colorimetric Ellman assay *(13)* was used for the determination of enzyme kinetics. The substrate solution contained 500 μ*M* acetylthiocholine iodide and 1 m*M* 5,5'-dithio-bis(2-nitrobenzoic acid) in 50 m*M* sodium phosphate buffer, pH 8.0. The microplates were read at 405 nm in the kinetic mode of a Molecular Devices Thermomax microplate reader at room temperature. All assay materials were obtained from Sigma.

Analysis of Enzyme Kinetics

Kinetic constants were determined by measuring the rate of the enzyme reaction in the presence of varying concentrations of PD 142676 and substrate (acetylthiocholine iodide). The results were displayed as Lineweaver-Burk (double-reciprocal) plots. Calculations for determining the maximal velocity of the enzyme reaction (V_{max}) and the affinity of the enzyme for the substrate (Km) were done using GRAFIT software (Sigma) *(14)*. Inhibition constants were determined by the method of Duggleby *(15)* provided in GRAFIT.

Dilution Experiments

Reversbility of AChE inhibition by PD 142676 was determined by dilution. Eel AChE (3.3 U) was added to 1 mL of 50 m*M* sodium phosphate buffer, pH 8.0, and incubated with various inhibitor concentrations for 15 min at room temperature. A 10-μL aliquot of each mixture was diluted 1:100 and then 1:10 to begin the radiometric enzyme assay (final enzyme dilution 1:1000). The enzyme activity of inhibitor-treated samples was divided by that of controls (no inhibitor) and then multiplied by 100 to determine the percent of total (control) AChE activity in the experimental group.

AChE Protection Assay

Diisopropyl fluorophosphate (DFP) and methanesulfonyl fluoride (MSF) were used to phosphorylate or to sulfonylate, respectively, the catalytically active serine in the active site of AChE. Reversible inhibitors can prevent irreversible inhibition if they bind near the active site and sterically protect the catalytically active serine.

Eel AChE (3.3 U) was added to 1 mL of 50 m*M* sodium phosphate buffer, pH 8.0, with various reversible inhibitor concentrations. After incubation at room temperature for 10 min, a 10-μL aliquot of each mixture was diluted 1:100 and then 1:10 at the time of AChE assay to determine if carryover of reversible inhibitor affected enzyme activity after dilution (carryover control). Then, the irreversible inhibitor DFP or MSF was added to 1 mL of each mixture for a final concentration of 10 μ*M* and 1 m*M*, respectively, to initiate the protection assay. After 30 min, a 10-μL aliquot of each mixture was diluted 1:100 followed by a 1:10 dilution (final dilution 1:1000) to start the radiometric enzyme assay. Thorough mixing was required at each step of this procedure.

The enzyme activity of inhibitor-treated samples was divided by that of controls (no reversible and no irreversible inhibitor) and then multiplied by 100 to determine the percent of total (control) AChE activity in the experimental group.

Phosphatidylinositol (PI) Turnover Studies

The assay was done as described previously *(16)*. Hm1 Chinese hamster ovary (CHO) cells were labeled with 1 μCi/mL of [^{3}H]-myo-inositol (SA = 15–18.8 Ci/mmol from NEN) in 0.5 mL of media/well. After 48 h, the medium was aspirated and the cells were washed two times with 1 mL minimum essential medium (MEM) containing 10 m*M* LiCl. One half of a milliliter MEM/LiCl was then added to each well and allowed to incubate at 37°C for at least 15 min. The stimulation period was initiated by the addition of 10 μL of the appropriate agonist concentration and allowed to proceed for 15 min, at which time the reaction was terminated by the aspiration of medium and the addition of 0.5 mL ice-cold 5% trichloroacetic acid (TCA). For antagonist experiments, compounds were added 5 min prior to the addition of 5 μ*M* carbachol. After waiting at least 15 min, the TCA extract was applied to Dowex-formate columns (Biorad AG 1-X8 resin, formate form, 100–200 mesh). The wells were rinsed

with 0.5 mL distilled H_2O and also applied to the columns. The columns were washed 4 times with 3 mL 5 m*M* myo-inositol and then total [^{3}H]-inositol phosphates were eluted into vials with two 2-mL washes of 1 m*M* ammonium formate containing 0.1*M* formic acid. Beckman Ready Gel scintillation cocktail (10 mL) was added and the samples counted in a Beckman 2800 scintillation counter. As an index of efficacy, the percent of maximal carbachol (1 m*M*) stimulation was calculated, while as a measure of inhibition, the concentration producing a half maximal response (IC_{50}) was calculated.

Muscarinic Receptor Binding Assay

Freshly dissected rat neocortex was homogenized in ice-cold 10 m*M* phosphate buffer (pH 7.4) using a Brinkman polytron at setting 5.5 and was used immediately for receptor binding assays. Antagonist binding assays were performed using procedures already described *(17)*. Antagonist sites of muscarinic receptors were labeled using [^{3}H]quinuclidinylbenzilate (QNB: final concentration 0.030–0.050 n*M*) in membrane preparations from cells or tissue homogenates. Incubations were conducted at 25°C for 2 h in a volume of 2 mL. Agonist binding assays were performed using methods similar to those described previously *(18)*. Agonist sites of muscarinic receptors were labeled using [^{3}H]-cis-methyldioxolane (CMD: final concentration 1 n*M*). Incubations were performed as described for [^{3}H]-QNB in glass tubes. For both ligands, nonspecific binding was determined in the presence of atropine (1 μ*M*). Eight to sixteen concentrations of competing ligand were used in displacement experiments. The amount of protein in each binding experiment varied depending on the ligand and tissue source. Protein concentrations were determined by the Pierce Bicinchoninic acid microtiter assay *(19)*. Binding assays were terminated by vacuum filtration over Whatman GF1B filters presoaked in 0.05% polyethylenimine using a Brandel cell harvester and washing 3–5 times with 2 mL of ice-cold phosphate buffer. The filters were counted in 7.5 mL of Ready Protein Plus Scintillation cocktail (Brinkman). Specifically bound [^{3}H]-QNB or [^{3}H]-CMD were calculated by subtracting nonspecific from total [^{3}H]-QNB or [^{3}H]-CMD bound. Free ligand concentration was calculated by subtracting total bound from total added. The IC_{50} values from competition experiments were determined from Hill plots.

In Vivo Microdialysis

Our animal studies were conducted according to the Declaration of Helsinki and with the Guide for the Care and Use of Laboratory Animals as adopted and promulgated by the National Institutes of Health. Housing facilities were accredited by the American Association for the Accreditation of Laboratory Animal Care.

The determination of extracellular levels of ACh in rat brain was done using methods similar to those already described *(20,21)*. Male Long-Evans rats weighing 250–400 g were anesthetized with 1.5 g/kg of urethane and placed securely into a stereotaxic frame. The nose elevation bar was set to zero. An incision was made in the skin, and the fascia were pinned away from the target zone using hemostats. An oblong hole was drilled in the skull, the dimensions of which approximated 1 mm left of center to 7 mm right of center and from bregma to 4 mm anterior. The dura were then pierced. A microdialysis probe (BioAnalytical Systems, Inc., CMA10 probe, MF 5143) measuring 0.5 mm OD by 20 mm in length with a dialysis membrane tip of 2 mm, was inserted into frontal cortex at coordinates 1 mm lateral to midline, 2 mm anterior to Bregma, at a 50° angle from medial to lateral, to a depth of 3 mm from the insertion point on the cortical surface. The recovery of the probes ranged from 10–20%.

The probe was perfused at a rate of 2 μL/min with artificial cerebral spinal fluid, containing 1.2 m*M* $CaCl_2$, 147 m*M* NaCl, and 4.02 m*M* KCl. Collection of dialysate was begun after a 2-h stabilization period. The dialysate was collected in plastic 1.5 mL Eppendorf tubes on ice over 1-h intervals for 5 h. The first sample was considered "baseline" and was subtracted from all subsequent experimental measurements to normalize values. The animals were then injected subcutaneously with *N*-methylscopolamine (0.32 mg/kg) in combination with either sterile water or PD 142676 (10.0 and 17.8 mg/kg). The *N*-methylscopolamine was used to block peripheral cholinergic side effects and had no effect itself on ACh levels. The order of drug treatment was randomized. A total of 8 animals were used for each possible combination. At the end of each 1-h collection period, 30 μL of acetylthiocholine was added to a final concentration of 200 ng/mL as an internal standard and 75 μL of each sample was immediately injected onto a Waters HPLC at a pump speed of 1 mL/min. The remain-

ing sample (75 µL) was frozen at –70°C for future analysis.

The mobile phase for the HPLC consisted of 50 m*M* sodium phosphate buffer at pH 8.5, with 5 mL/L Kathon as an antibacterial agent. The ACh was detected using the BAS Acetylcholine detection kit, following the manufacturer's directions for electrochemical detection. The hydrogen peroxide produced by the reaction was measured by electrochemical detection using a Waters 464 Electrochemical Detector with a platinum working electrode set at +0.5 V vs the Ag/AgCl reference electrode. The data was captured by computer using the BASELINE chromatography software system and was analyzed by comparing the response of unknown samples to a standard curve produced with known concentrations of ACh.

The remaining 75 µL of dialysate was tested for anticholinesterase activity using a radiometric AChE assay. Seventy-five microliters of dialysate was diluted with 25 µL of [^{3}H]-ACh to a final concentration of 0.1 µCi/100 µL. A 10-µL Aliquot of Sigma human red blood cell AChE (Type XIII), diluted 1:500, was added to the mixture. The reaction was stopped after 15 min. The amount of enzyme inhibition was determined by dividing the enzyme activity of samples by the activity of controls (dialysate from animals with no anticholinesterase treatment) and multiplying by 100. A standard curve of enzyme inhibition, produced by known amounts of anticholinesterase, was used to estimate the amount of inhibitor in the dialysate.

Mouse Water-Maze Test

C57BL/10SnJ (B10) mice were selected on the basis of strain differences in neuron number and volume of the hippocampus with B10 mice having a smaller hippocampus than other inbred strains *(22)*, and previous work demonstrating poor performance of these mice in a water maze task *(23)*. Performance of these mice was tested in a square water-maze measuring 61 × 61 × 30.5 cm, filled to a depth of 11.5 cm with a mixture of water (21–23°C) and 1.5 g/L of instant dry milk. A small moveable platform (7.62 cm square on top) was located in one quadrant of the maze. The top of the platform was 1 cm below the surface of the water. Latency to find the hidden platform served as the dependent measure. Testing was conducted over 2 d with 4 trials conducted each day. The starting location was randomly blocked across trials so that mice were started once from each corner of the maze on each test day. A trial consisted of facing the animal into a corner of the maze, releasing it, and then measuring the latency to climb onto the platform or until 2 min elapsed. The mouse was then towel dried, placed into a holding cage for 30 s, and returned to the maze for the next trial. Between test days mice were housed in their home cage in the testing room. Seven to twenty-eight mice were studied at each dose level over 4 separate replications. Each replication included 5 groups (vehicle, tacrine 10.0 mg/kg, and 3 doses of PD 142676) with 7 animals in each group. Not all doses of PD 142676 were studied in each replication. Drug or vehicle was administered 30 min before testing on each test day. Data were analyzed using one-way analysis of variance followed by Newman-Keuls post hoc comparisons. Data from each test day were analyzed separately.

Aged Monkey Delayed Match-to-Sample

The subjects were drug and test-sophisticated aged rhesus monkeys (over 25-yr-old, two males and five females). These animals were fed (Certified Primate Chow #5045) full rations 16–20 h before testing and were maintained on a 12-h light-dark cycle in a vivarium adjoining the test room. Monkeys were transported from the vivarium to the testing chambers in specially designed transport cages that they freely entered and exited. This permitted freely moving animals, without physical restraint and direct human contact.

Performance on a match-to-sample task was measured using a microcomputer-controlled test environment. In this test, a sample object (a solid-colored red square, yellow diamond, or blue circle) was displayed against a black background on the screen of a color television monitor (CRT). The sample was presented in the center top third of the CRT screen for 2 s. Each object served as the sample once every three trials in a randomized complete block design. This test was self-paced with sample presentations initiated when the monkey interrupted a photobeam by moving its head through an opening in a black acrylic barrier located 20 cm in front of the center of the CRT screen. The monkey was required to break the photobeam throughout the 2-s presentation. Following sample presentation, the CRT screen was cleared to black and a delay interval of varying lengths ensued. Recall of the correct sample object was tested following retention intervals of varying lengths (0, short: 1 s, long: 5–15 s). The long delay was

titrated to a performance criterion of 50% correct, determined individually for each monkey. Duration of the delay was determined by a randomized complete block design with retention intervals selected such that each delay occurred once every three trials. The delay interval was signaled by a tone (700 Hz, 500 ms) as each second counted down. After this delay, all three sample objects (red square, yellow diamond, and blue circle) were displayed in a row (in random order) across the bottom third of the CRT screen against a black background. The order of these stimuli was changed from trial to trial. A correct response consisted of the monkey touching the CRT screen in the spatial location covered by the correct sample object. Responses (touching the CRT screen) were detected by an array of photocells located around the perimeter of the CRT (Carroll Touch Technology) and connected to microcircuitry that returned the spatial location in x,y coordinates to the microcomputer. Correct responses were rewarded by delivery of a 190-mg banana-flavored food pellet and presentation of an ascending tone series (500 ms duration). Incorrect responses were signaled by a 700 Hz tone (500 ms) but were not rewarded. After a response, the CRT screen was cleared to black and a two second intertrial interval ensued, after which the monkey could initiate the next trial. Each test session consisted of 85 trials. All testing was conducted in sound-attenuating chambers (Industrial Acoustics) with background noise provided by cooling fans and illumination provided by an overhead houselight.

Monkeys exhibited stable performance on the delayed-match-to-sample task for at least 2 yr before this experiment. These monkeys were drug-experienced, but they had not received cholinomimetic treatment for at least 30 d before this experiment. In this experiment monkeys received PD 142676 (0.03, 0.1, 0.3, and 1.0 mg/kg) or vehicle (0.9% saline) intramuscularly 30 min before testing. Each monkey received all treatments in counter-balanced order over 5 test sessions across 3 wk. Drug was administered only on test days and test days were separated by at least 48 h. Drug effects were evaluated by comparing the mean percent-correct performance at the zero second (nonmemory) and all nonzero second delays (memory) under drug and vehicle conditions. Because of large interanimal variation in baseline performance, data were analyzed using paired t-tests. Difference scores were calculated between vehicle and drug treatments for each dose at each delay.

Determination of Core Body Temperature

PD 142676 (10.0, 17.8, 32.0, or 100.0 mg/kg) or vehicle (2% carboxymethylcellulose) was administered by gavage 15 min before testing. Body temperature was recorded through a rectal probe.

Quantitative Electroencephalography (QEEG)

Male Long-Evan rats weighing 350–500 g were surgically implanted with stainless steel electrodes screwed into the skull surface overlying the frontal and occipital cortex. Electrodes were secured to a plastic connector (Plastic Products Model MS-363) that was permanently attached to the skull surface with dental acrylic. Animals were given 1 wk to recover from surgery before testing. After recovering from surgery, animals were placed into sound attenuating chambers during the light cycles of the rat's diurnal cycle. Animals were allowed 2 h to habituate to these environments. Thereafter, EEG was recorded continuously for 20 min before and 4 h after drug administration. Every other 1-s sample of EEG was converted from the time to the frequency domain using a fast Fourier transformation (FFT). The power spectra from these FFTs were summed across 15-min epochs to yield a mean power spectrum for the period. Mean power within the 0–4 (delta), 5–8 (theta), 9–5 (alpha), and 16–25 (beta) Hz bands was calculated separately for each bandwidth. Total power within all bandwidths also was calculated. Data from each bandwidth and total power were analyzed separately using nonparametric ranked analysis of variance (Kruskals-Wallis rank transformed analysis with repeated measures). Comparisons among means were made using Duncan's post hoc tests at inclusive intervals prior to treatment and at 15–30, 45–60, 60–90, and 90–120 min after drug administration.

PD 142676 (3.2, 10.0, and 32.0 mg/kg) or vehicle (2% carboxymethylcellulose) was administered by gavage. Treatments were given in random order with no more than two treatments a week and at least 2 d separating treatments.

Determination of Gastrointestinal (GI) Motility

Male Long-Evans rats weighing 150–200 g were fasted for 38–48 h before the experiment with water available ad libitum. Fasted rats were then injected by gavage with 20 red dacron pellets (1/16 in. in

diameter, Small Parts, Inc.). Rats were killed by cervical dislocation 2 h after pellet gavage. Their stomachs and small intestines were removed, and aligned on a calibrated light table. The pellets in the lumen of the intestine and stomach were counted and the distance traveled by each pellet was recorded. Data were evaluated by calculating the percentage of pellets entering the intestines (stomach emptying) and the distance traveled by the leading pellet (intestinal transit). PD 142676 (10.0, 32.0, and 100.0 mg/kg) or vehicle (2% to carboxymethylcellulose) was injected immediately prior to introduction of pellets to the stomach.

In separate experiments to determine the effects of muscarinic angonists on GI motility, rats were killed by cervical dislocation 20 min after pellet gavage and treatment with the balanced muscarinic agonist CI 979 (1.0 and 3.2 mg/kg) administered in combination with PD 142676 (0.0, 3.2, 10.0, and 32.0 mg/kg) 15 min before introduction of pellets to the stomach.

Results

PD 142676 Inhibition of AChE

PD 142676 is a potent, reversible inhibitor of AChE. The inhibitory potency of PD 142676 compares favorably to other anticholinesterases being considered for the treatment of AD. Determinations of IC_{50} values against human AChE reveal that PD 142676 has a potency as an anticholinesterase comparable to other compounds under development (Table 1). PD 142676 is almost equipotent with tacrine in inhibiting AChE, but less potent than tacrine in inhibiting BuChE (Table 1). Under our assay conditions, the most potent anticholinesterase tested is E2020, and the least potent is velnacrine (HP-029, Mentane®). PD 142676 is a reversible inhibitor of AChE, as determined by a dilution assay. Sufficiently diluting the reversible inhibitor-enzyme mixture fully recovers AChE activity. In contrast, an irreversible inhibitor continues to inhibit the enzyme regardless of dilution. Mixing eel AChE in up to 10 μ*M* PD 142676 followed by 1000-fold dilution results in AChE activity equal to that of controls (data not shown).

PD 142676 produces mixed inhibition of AChE by binding to the active site of the enzyme. An enzyme kinetic analysis of human AChE in the presence of increasing concentrations of inhibitor shows that PD 142676 is a linear mixed inhibitor (Fig. 1). PD 142676 competitively reduces the affinity of the enzyme for the substrate (decreases Km) and noncompetitively slows the velocity of substrate hydrolysis (decreases V_{max}). The inhibition constant for the competitive component of the inhibition (Kis) is about 45 n*M*, slightly lower than the inhibition constant for the noncompetitive component (Kii), 81 n*M*. Mixed inhibitors can bind to one of two sites on AChE, either in the active site or at a site peripheral to the active site *(24–27)*. Inhibitors that bind to the peripheral site (e.g., propidium) only partially protect AChE from DFP, and not at all against MSF. In contrast, active site inhibitors can totally protect the enzyme from DFP and sometimes partially against MSF (e.g., edrophonium) *(26,27)*. PD 142676 at concentrations of 10 μ*M* totally protects AChE from irreversible inhibition by the organophosphate DFP, but not the physically smaller organosulfonate MSF (Fig. 2). This implies that PD 142676 binds in the active site of AChE, but not close enough to protect the catalytically active serine from irreversible inhibition by MSF.

Table 1
Comparison of Cholinesterase Inhibition by PD 142676 and Other Anticholinesterases[a]

Common name	IC_{50} human AChE, n*M*	IC_{50} horse BuChE, n*M*
E2020	2	4166
SM-10888	25	17.3
Tacrine	30	5.2
PD 142676	40	20000
Galanthamine	100	7167
Heptyl-physostigmine	125	34.3
(±) Huperzine A	150	66667
Velnacrine (HP-029)	200	53.3

[a]The data represent the mean of radiometric AChE assays or BuChE colorimetric assays done in triplicate. The standard error for each value is ≤10% of the mean.

PD 142676 Interacts with Muscarinic Receptors

PD 142676 has properties of a functional muscarinic antagonist. PD 142676 displaces the binding of the muscarinic agonist CMD (IC_{50} = 209 n*M*) and the muscarinic antagonist QNB (IC_{50} = 398 n*M*) from rat neocortex membranes. The amount of PD 142676 needed for displacement of ligand binding to muscarinic receptors is higher than needed to inhibit rat brain AChE (IC_{50} = 65 n*M* as determined by the radiometric AChE assay). The ratio of the displacement of QNB and CMD (QNB/CMD) is 1.9,

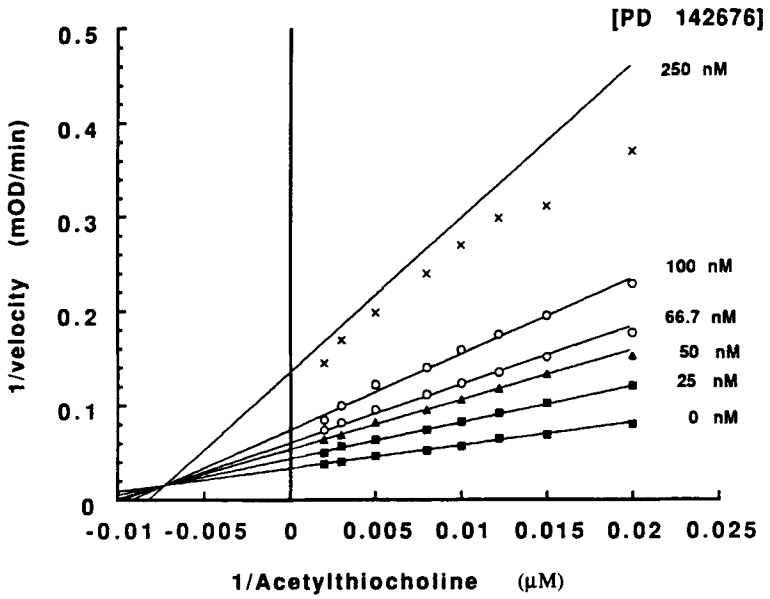

Fig. 1. Double-reciprocal plots for inhibition by PD 142676 of acetylthiocholine hydrolysis by human red blood cell AChE.

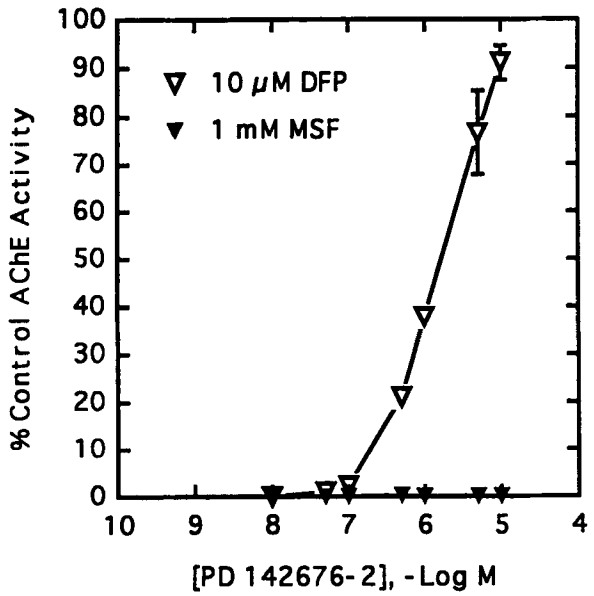

Fig. 2. PD 142676 protection of eel AChE from irreversible inhibition. The values are the means ± SE (n = 3 for each value).

a ratio produced by other known muscarinic antagonists (e.g., scopolamine) in this assay. The physiological responses to PD 142676 further suggest that the compound acts as a muscarinic antagonist. Stimulation of Hm 1 CHO cells with carbachol produces increased receptor-linked phosphatidylinositol (PI) turnover. PD 142676 inhibits carbachol-induced PI turnover (Fig. 3) with an IC_{50} of 1.6 μM, confirming that the compound has the properties of a functional muscarinic antagonist. Muscarinic antagonism is also evident in animals. Gastric motility in rats decreases in a dose-dependent manner after oral administration of PD 142676 (Fig. 4). This is in marked contrast to the increased gastric motility produced by tacrine in this species (data not shown). Administration of the balanced muscarinic agonist CI 979 increases gastric motility and this action is competitively inhibited by PD 142676 (Fig. 5). Thus, PD 142676 appears to be an anticholinesterase and at higher concentrations a functional muscarinic antagonist.

PD 142676 Is a Centrally Acting Cholinomimetic

The cholinomimetic actions of PD 142676 dominate centrally. Orally administered PD 142676 produces a dose-dependent decrease in the total power of the cortical EEG activity in rats (Fig. 6). The response indicates an alert or awake state, and is typical of the effects of other centrally active cholinomimetics (e.g., anticholinesterases and muscarinic agonists). Similar effects occur in EEG recordings from rhesus monkeys (data not shown). Oral administration of PD 142676 produces a

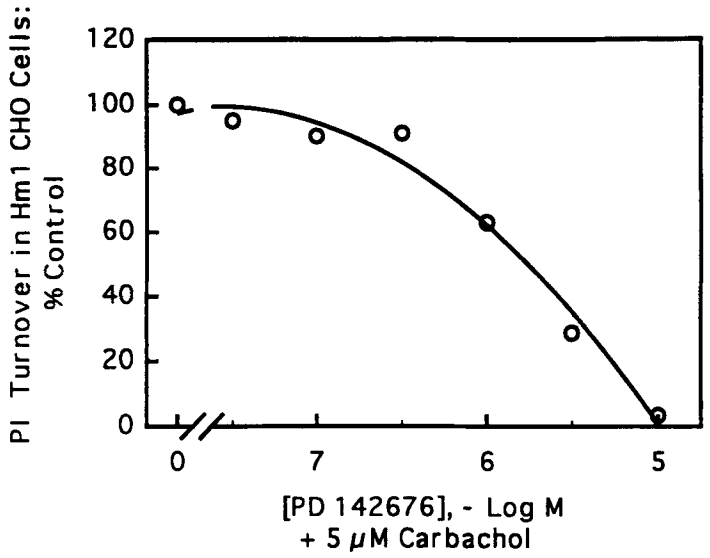

Fig. 3. Effects of PD 142676 on carbachol-induced PI-turnover in Hm1 CHO cells. The values are the mean ± SE (n = 3 for each value).

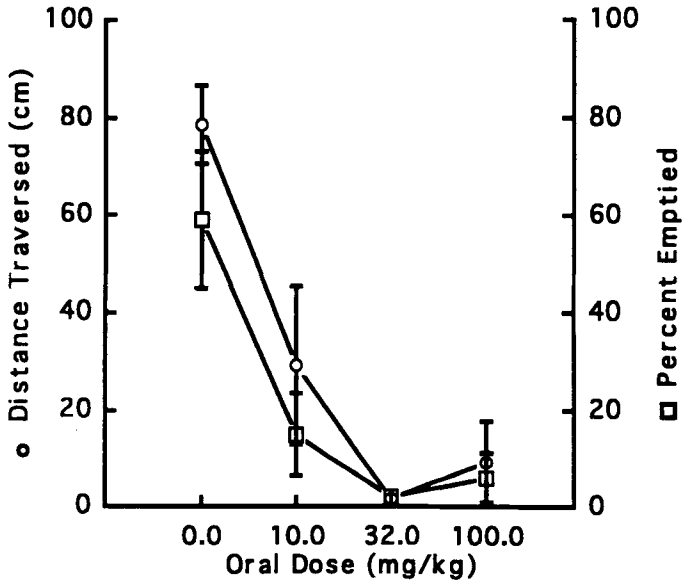

Fig. 4. PD 142676 decreases gastric motility in rats. The values are the means ± SE (n = 5/dose).

decrease in core body temperature in rats (Fig. 7). Other anticholinesterases and muscarinic agonists also produce this effect (e.g., tacrine). Thus, despite being a muscarinic antagonist peripherally at high doses, PD 142676 is able to enhance central cholinergic function in a manner similar to other anticholinesterases in both rodents and monkeys.

Increased ACh levels mediate the cholinomimetic effects of PD 142676. ACh levels in brain were monitored by in vivo microdialysis. Subcutaneously administered PD 142676 increases the levels of cortical ACh in anesthetized rats between two- to threefold over basal levels. The increase is dose- and time-dependent (Fig. 8A) with the peak level being reached by 3 h. The anticholinesterase activity in the dialysates also increases in parallel with ACh levels (Fig. 8B), implying the presence of PD 142676 or active

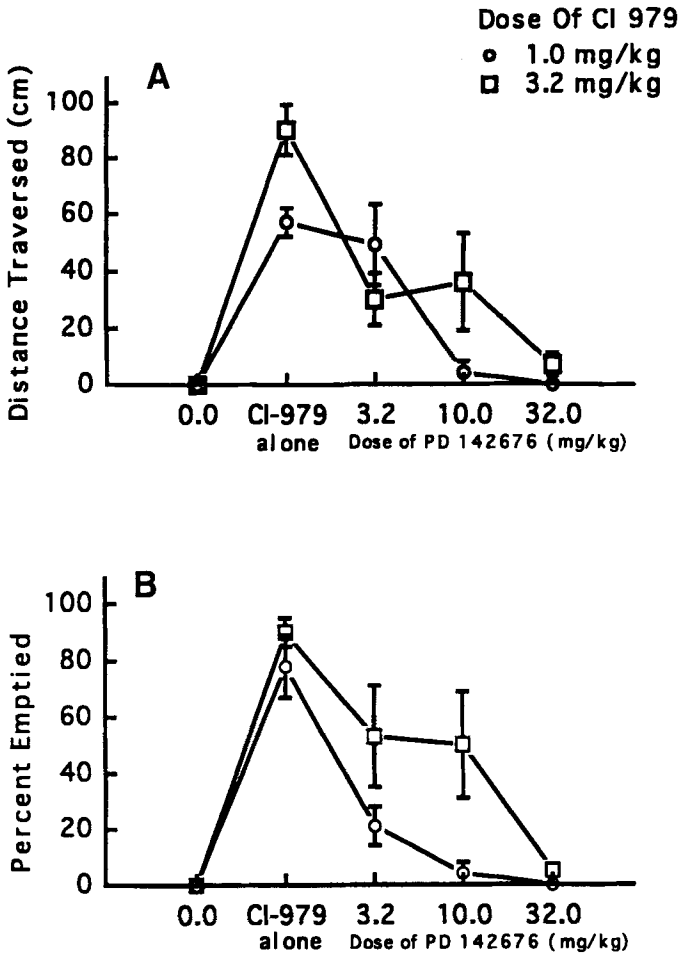

Fig. 5. CI 979 antagonism of PD 142676 inhibition of gastric motility in rats. **(A)** Effects of PD 142676 on the distance travelled by pellets. **(B)** Effects of PD 142676 on stomach emptying. The values are the means ± SE (n = 5/dose).

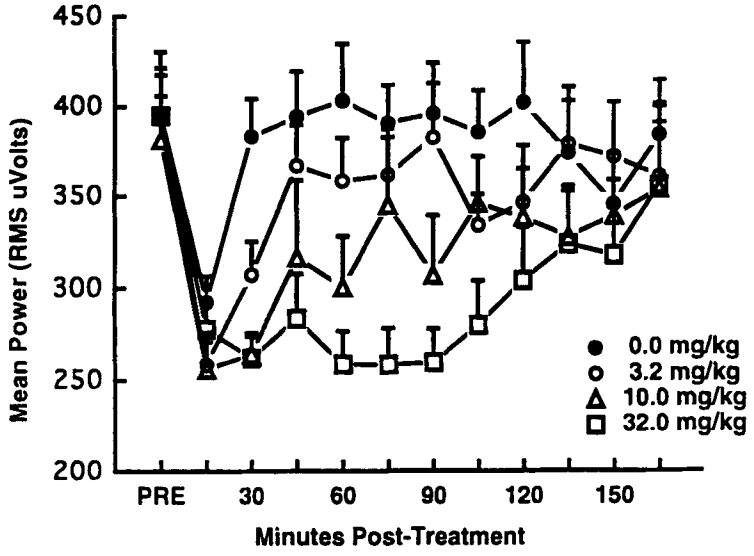

Fig. 6. PD 142676 decreases total power in rat cortical QEEG. The values are the means ± SE (n = 8/ dose).

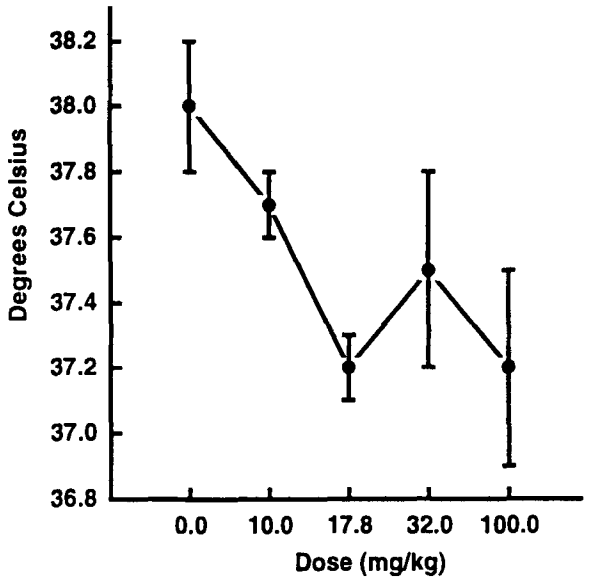

Fig. 7. Decrease in core body temperature produced by PD 142676 in rats. The values are the means ± SE (n = 7/ dose).

metabolites in the extracellular environment of the frontal cortex.

PD 142676 Improves Cognitive Performance

PD 142676 also improves the performance of C57/B10j mice in the mouse water maze test. Significant improvement occurs following the 17.8 mg/kg dose of PD 142676 on the second test day (Fig. 9). This compares favorably with the best dose of tacrine (10.0 mg/ kg) (Fig. 9). The performance of aged rhesus monkeys on a delayed match-to-sample task also improves after treatment with PD 142676 (Fig. 10). Significant enhancement of delayed match-to-sample performance occurs at the long-delay after 0.1 m/kg (IM) of PD 142676. At this dose, aged monkeys perform as well on trials with long-delay (>5 s) as those with short-delays (< 5 s). Five of seven monkeys showed dramatic improvement whereas the other two monkeys were not improved at the 0.1 mg/kg dose. Thus, PD 142676 improves cognitive performance in monkeys and rodents.

Discussion

The cholinergic deficit associated with AD prompted the testing of anticholinesterases in an effort to restore diminished cholinergic function in the central nervous system. Early results using this

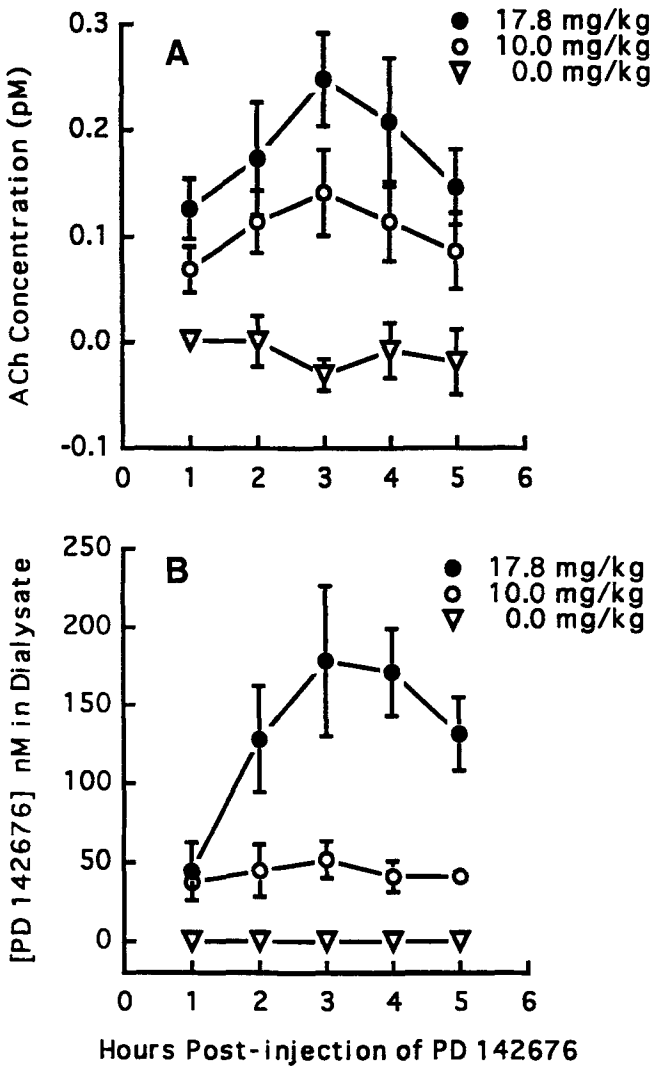

Fig. 8. Determination of ACh concentrations and anticholinesterase activities in microdialysis samples from the frontal cortex of rats treated with PD 142676. **(A)** ACh levels are the mean ± SE (n = 8/dose). **(B)** The anticholinesterase activities are the mean ± SE (n = 3/ dose).

replacement therapy approach with physostigmine were promising, but only recent clinical studies with the anticholinesterase tacrine have validated the approach. This success has now challenged us to develop even better anticholinesterases, designed specifically for the manipulation of cholinergic function in the brain, but without unwanted side effects. Thus far, our efforts have yielded a novel anticholinesterase, PD 142676.

Our analysis shows that PD 142676 is a potent, reversible inhibitor of AChE. This anticholinesterase binds to the active site, but there is no associa-

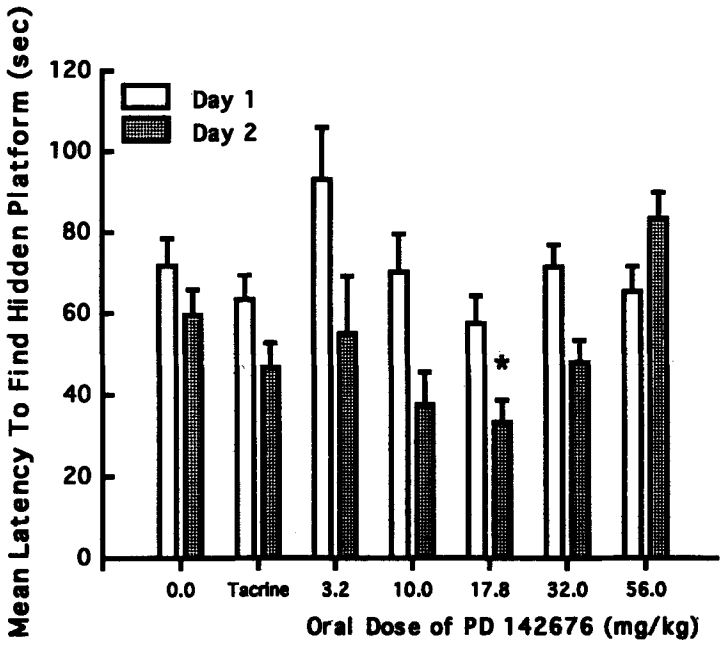

Fig. 9. PD 142676 significantly improves performance at 17.8 mg/kg on the second day of testing in the mouse water-maze. The values are the means ± SE (n = 7–28 mice at each dose). *$p < 0.05$, Newman-Keuls post hoc comparison, drug vs vehicle.

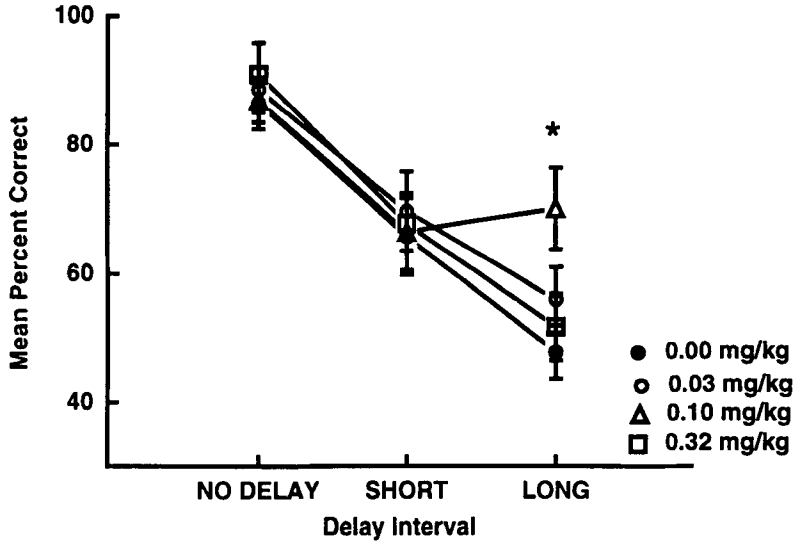

Fig. 10. PD 142676 at 0.01 mg/kg improves group performance of aged monkeys on trials with long delays in a delayed match-to-sample task. The values are the means ± SE (n = 7/dose). *p <0.05, paired t-test.

tion with the catalytically active serine. The inhibition of AChE by PD 142676 is readily and rapidly reversible, unlike longer-acting (irreversible) anticholinesterases, such as carbamates and organophosphates. This noncovalent interaction produces a mixed (competitive and noncompetitive) inhibition of enzyme activity. PD 142676 competitively competes with ACh binding to the active site of AChE. It also noncompetitively associates with the acyl-enzyme intermediate of AChE, slowing the rate of deacetylation and consequently reducing the velocity of ACh hydrolysis *(28)*. An advantage of mixed inhibitors over purely competitive inhibitors is that the effectiveness of the noncompetitive com-

ponent remains unchanged as ACh levels rise. In contrast, increasing the concentration of ACh reduces the effectiveness of a purely competitive inhibitor. Thus, mixed inhibitors of AChE may have an advantage in producing and maintaining higher levels of brain ACh than purely competitive anticholinesterases of similar potency. Moreover, the effect of mixed inhibition on AChE activity is readily reversible. The reversibility of AChE activity is not dependent on chemical reactivation or on replenishment of AChE through de novo synthesis that is necessary after inhibition by irreversible inhibitors. Therefore, the action of PD 142676 should be readily reversible in the clinical setting, a distinct advantage over irreversible inhibitors.

The enzyme inhibition caused by PD 142676 is similar to tacrine, which is also a reversible, mixed, active site inhibitor of AChE *(26,27,29,30)*. Although the aminoacridine tacrine inspired the design of PD 142676, our results show that the pharmacological profile of the dihydroquinazoline differs from its predecessor in several respects. Unlike tacrine, PD 142676 is a poor inhibitor of BuChE. This lack of BuChE inhibition appears not to diminish the effectiveness of PD 142676 as a cognitive enhancer. Conversely, this implies that the potency of tacrine in inhibiting BuChE is not critical for its effects on cognitive function. This result is consistent with the fact that BuChE has, at best, a modest physiological role in cholinergic function. PD 142676 is also a functional muscarinic antagonist, whereas tacrine is not. The antagonism occurs at higher concentrations of PD 142676 than needed to inhibit AChE. In vivo, PD 142676 antagonizes muscarinic functions peripherally, as revealed by decreased gastrointestinal motility in rats. We have yet to find other indications of peripheral cholinergic antagonism (i.e., decreased glandular secretions and micturition or increased heart rate) even at doses (90 mg/kg in rodents, 75 mg/kg in monkeys) substantially above those required to improve cognitive function, implying that PD 142676 may act as a muscarinic antagonist only at certain sites in the periphery.

Despite its antagonist properties, PD 142676 acts as a cholinomimetic centrally. Reductions in core body temperature and increases in cortical electrical activity are evidence of its central cholinergic effects. Increased levels of brain ACh, as measured by microdialysis, appear to mediate these changes. Most important is that these pharmacological and physiological effects lead to improved cognitive performance in both rodents and monkeys. PD 142676 is as efficacious as, or better than, tacrine in improving cognition in these tests. Thus, our findings establish PD 142676 as a centrally active, orally available cholinomimetic with cognition enhancing properties.

Our characterization of PD 142676 shows that it is unique among the AChE inhibitors currently undergoing evaluation as potential treatments for AD. Unlike other anticholinesterases, PD 142676 acts as a muscarinic antagonist in the gastrointestinal tract and this may limit peripheral cholinergic side effects. The antagonism reduces gastric motility in animals, suggesting that it may be useful in mitigating the nausea and diarrhea experienced by humans treated with other anticholinesterases. Thus far, we have not observed any untoward effects of PD 142676 on other peripheral cholinergic functions. Thus, in several respects PD 142676 may be an improvement over conventional anticholinesterases. An issue to resolve is if PD 142676 produces any changes in the serum level of liver enzymes in humans. Unfortunately, there is no model (animal or in vitro) that can predict the hepatic effects, if any, of PD 142676. Our expectation is that by virtue of its different chemical structure, PD 142676 will not produce tacrine-like changes in the serum level of liver-derived aminotansferases. However, the answer to this question must wait until results from human clinical testing.

The primary effect of anticholinesterase treatment in AD is expected to be palliative, mediated by increased efficacy of chemical transmission at cholinergic synapses. However, recent results suggest that a cholinomimetic may also influence the production of the amyloid precursor protein (APP) and possibly even the β-amyloid peptide (A/β4). Nitsch and his colleagues *(31)* recently showed in cell culture studies that cholinergic agonists increase the secretion of APP from cells with m1 and m3 muscarinic receptors. The secretion is mediated by an unidentified protease (APP secretase) that cleaves full-length APP in the middle of its A/β4 region *(32,33)*, rendering the products nonamyloidogenic. We *(34)* and others *(35,36)* have replicated these findings on the effects of muscarinic agonist-induced APP secretion.

Stimulation of this type of APP processing could prove beneficial in the treatment of AD. It is possible that the amount of full-length APP available for processing by the amyloidogenic pathway would be reduced on stimulation of m1 or m3

cholinociceptive cells. In turn, this could reduce the rate of A/β4 production and, consequently, formation of amyloid plaques. The secreted APP may also be neuroprotective. Glutamate toxicity is reduced in cultured nerve cells treated with APP *(37)*. These effects on and by APP have yet to be demonstrated in vivo. However, it is intriguing to speculate that cholinomimetics may alter APP processing in hippocampus and cortex where m1 and m3 receptors are present *(38)*. It is equally thought-provoking to consider the possibility that the production of A/β4 might be related to the decline in cholinergic innervation evident in AD brains. This reduced cholinergic activity may also explain the lower levels of APP in the cerebral spinal fluid of AD patients compared to age-matched controls *(39)*. Whether or not the relationships exist between cholinergic activity, Aβ4 production, and the pathogenesis of AD remains to be determined. However, application of this hypothesis to future research may provide the linkage between the cholinergic and amyloid hypotheses of AD, and stimulate greater insights into the therapeutic opportunities that exist for AD treatment.

References

1. Moos W. H., Davis R. E., Schwarz R. D., and Gamzu E. R. (1988) *Med. Res. Rev.* **8,** 353–391.
2. Joachim C. L. and Selkoe D. J. (1992) *Alzheimer's Dis. and Assoc. Dis.* **6,** 7–34.
3. Davis R. E., Emmerling M. R., Jaen J. C., Moos W. H., and Spiegel K. (1993) *Crit. Rev. Neurobiol.* **7,** 41–83.
4. Giacobini E. and Becker R. (1989) *Prog. Clin. Biol. Res.* **317,** 1121–1154.
5. Palacios J. M. (1993) *Curr. Opin. Invest. Drugs* **2,** 379–386.
6. Kumar V. and Calache M. (1991) *Int. J. Clin. Pharm. Ther. Tox.* **29,** 23–37.
7. Davis K. L., Thal L. J., Gamzu E. R., Davis C. S., Woolson R. F., Gracon S. I., Drachman D. A., Schneider L. S., Whitehouse P. J., Hoover T. I., Morris J. C., Kawas C. H., Knopman D. S., Earl N. L., Kumar V., and Doody R. S. (1992) *New Engl. J. Med.* **327,** 1253–1259.
8. Farlow M., Gracon S. I., Hershey L. A., Lewis K. W., Sadowsky C. H., and Dolan-Ureno J. (1992) *JAMA* **268,** 2523–2529.
9. Freeman S. E. and Dawson R. M. (1991) *Prog. Neurobiol.* **36,** 257–299.
10. Jaen J. and Davis R. E. (1993) *Curr. Opin. Invest. Drugs* **2,** 363–377.
11. Johnson C. D. and Russell R. L. (1975) *Anal. Biochem.* **64,** 229–238.
12. Emmerling M. R. and Sobkowicz H. M. (1988) *Hearing Res.* **32,** 137–146.
13. Ashour A., Gee S. J., and Hammock B. D. (1987) *Anal. Biochem.* **166,** 353–360.
14. Leatherbarrow R. J. (1990) *GRAFIT Version 2.0.* Erithracus Software Ltd., Staines UK.
15. Duggleby R. G. (1988) *Med. Metab. Biol.* **40,** 204–212.
16. Berridge M. J., Downes C. P., and Hanley M. R. (1982) *Biochem. J.* **206,** 587–595.
17. Waeson M., Yamamura H., and Roeske W. R. (1986) *J. Pharmcol. Exp. Ther.* **237,** 411–418.
18. Vickroy T. W., Roeske W. R., and Yamamura H. I. (1984) *J. Pharmacol. Exp. Ther.* **229,** 747–753.
19. Smith P. K., Krohn R. I., Hermanson G. T., Mallia A. K., Gartner F. H., Pvenzano M. D., Fujimoeo E. K., Goeke N. M., Olson B. J., and Klenk D. C. (1985) *Anal. Biochem.* **150,** 76–85.
20. Ungetede U. (1987) *Life Sci.* **41,** 861–864.
21. Xu M., Nakamura Y., and Yamamoto T. (1991) *Neurosci. Lett.* **123,** 179–182.
22. Wimer R. E. and Wimer C. C. (1981) *Brain Res.* **254,** 129–140.
23. Symons J. P., Davis R. E., and Marriott J. G. (1988) *Life. Sci.* **42,** 375–383.
24. Mooser G. and Sigman D. S. (1974) *Biochemistry* **13,** 2299–2307.
25. Taylor P. and Lappi S. (1975) *Biochemistry* **14,** 1989–1997.
26. Moore C. J., Gregor V. E., Lee C., and Emmerling M. R. (1991) *Soc. Neurosci. Abstr.* **17,** 701.
27. Emmerling M. R., Moore C. J., Gregor V. E., and Lee C. (1991) *Soc. Neurosci. Abstr.* **17,** 701.
28. Krupka R. M. and Ladler K. J. (1961) *J. Am. Chem. Soc.* **83,** 1445–1447.
29. Berman H. A. and Leonard K. (1992) *Mol. Pharm.* **41,** 412–418.
30. Dawson R. M., Dowling M. H., and Poretski M. (1991) *Neurochem Int.* **19,** 125–133.
31. Nitsch R. M., Slack B. E., Wurlman R. J., and Growdon J. H. (1992) *Science* **258,** 304–307.
32. Anderson J. P., Chen Y., Kim K. S., and Robakis N. K. (1992) *J. Neurochem.* **59,** 2328–2331.
33. Weidemann A., Konig G., Bunke D., Fischer P., Salbaum J. M., Masters C. L., and Beyreuther K. (1989) *Cell* **57,** 115–126.
34. Doyle P. D., Moore C. J., Carroll R. T., Emmerling M. R., and Davis R. E. (1993) *Soc. Neurosci. Abstr.* **19,** 346.
35. Buxbaum J. D., Oishi M., Chen H. I., Pinkas-Kramarski R., Jaffee E. A., Gandy S. E., and Greengard P. (1992) *Proc. Natl. Acad. Sci.* **89,** 10,075–10,078.
36. Lahiri D. K., Nall C., and Farlow M. R. (1992) *Biochem. Int.* **28,** 853–860.
37. Mattson M. P., Lieberburg I., and Rydel R. (1992) *Soc. Neurosci. Abstr.* **18,** 1438.
38. Levey A. I., Kitt C. A., Simonds W. F., Price D. L., and Brann M. R. (1991) *J. Neurosci.* **11,** 3218–3226.
39. Van Nostrand W. E., Wagner S. L., Shankle W. R., Fanow J. S., Dick M., Rozemuller J. M., Kuiper M. A., Wolters E. C., Zimmerman J., Cotman C. W., and Cunningham D. D. (1992) *Proc. Natl. Acad Sci. USA* **89,** 2552–2555.